A Combined Quantum Mechanical and Statistical Mechanical Study of the Equilibrium of Trimethylaluminum (TMA) and Oligomers of $(AlOCH_3)_n$ Found in Methylaluminoxane (MAO) Solution

E. Zurek and T. Ziegler*

Department of Chemistry, University of Calgary, Calgary, Alberta, Canada, T2N 1N4

Received December 22, 2000

Density Functional Theory (DFT) has been used to calculate the energies of over 30 different structures with the general formula $(AlOMe)_n \cdot (AlMe_3)_m$ where n ranges from 6 to 13 and m ranges between 1 and 4, depending upon the structure of the parent $(AlOMe)_n$ cage. The way in which TMA (trimethylaluminum) bonds to MAO (methylaluminoxane) has been determined as well as the location of the acidic sites present in MAO caged structures. Topological arguments have been used to show that TMA does not bind to MAO cages where $n = 12$ or $n \geq 14$. The ADF energies in conjunction with frequency calculations based on molecular mechanics have been used to estimate the finite temperature enthalpies, entropies, and free energies of the TMA containing MAO structures. Using the Gibbs free energies found for pure MAO structures calculated in a previous work, in conjunction with the free energies of TMA containing MAO structures obtained in the present study, it was possible to determine the percent abundance of each TMA containing MAO within the temperature range of 198.15 K−598.15 K. We have found that very little TMA is actually bound to MAO. The Me/Al ratio on the MAO cages is determined as being approximately 1.00, 1.01, 1.02, and 1.03 at 198, 298, 398, and 598 K, respectively. Moreover, the percentage of Al found as TMA has been calculated as being 0.21%, 0.62%, 1.05%, and 1.76% and the average unit formulas of $(AlOMe)_{18.08} \cdot (TMA)_{0.04}$, $(AlOMe)_{17.04} \cdot (TMA)_{0.11}$, $(AlOMe)_{15.72} \cdot (TMA)_{0.17}$, and $(AlOMe)_{14.62} \cdot (TMA)_{0.26}$ have been determined at the aforementioned temperatures.

I. Introduction

In a previous work[1], we have studied the equilibrium between oligomers of $(AlOCH_3)_n$ which are present in a trimethylaluminum (TMA) free methylaluminoxane (MAO) solution. Our calculations show that "pure MAO" is composed of three-dimensional caged structures made up of alternating four-coordinate aluminum and three-coordinate oxygen atoms. Moreover, these caged structures consist only of square and hexagonal faces as first suggested by Barron.[2] The presence of octagonal faces destabilizes the structures as it adds more square faces, exhibiting high ring strain, to the cage. Within structures generated from hexagonal and square faces only, there are four bonding environments within which an atom may be found. That is, it can belong to three square faces (3S), two square and one hexagonal face (2S + H), two hexagonal and one square face (2H + S), or three hexagonal faces (3H). We have found that the stability of a given structure is dependent upon the "types" of atoms which are found in the caged compound. For example, the ring strain associated with an atom in a 3S environment is quite large. Hence, cages containing atoms in such environments were less energetically stable. The order of stability was found as being 3H > 2H + S > 2S + H > 3S.

We have also calculated a percent distribution of such $(AlOMe)_n$ structures within the temperature range of 198−598 K. This was used to obtain an average n value of 18.41, 17.23, 16.89, and 15.72 at 198, 298, 398, and 598 K, respectively. The percent distribution at different temperatures is given in Figure 1 and the most stable structure at all temperatures, $(AlOMe)_{12}$, is shown in Figure 2.

Controlled hydrolysis of TMA in toluene or other hydrocarbon solvent leaves residual TMA present in the MAO solution.[3] It is generally accepted that the TMA exists as the free and bound species according to the following equilibrium

$$(AlOMe)_n + \frac{m}{2}(Al(CH_3)_3)_2 \Leftrightarrow (AlOMe)_n \cdot (Al(CH_3)_3)_m \quad (1)$$

In the present study we examine the degree to which TMA is coordinated to MAO as well as the bonding mode of this coordination.

Several experimental attempts have been undertaken to establish the degree to which TMA is coordinated to MAO.[3−7] Moreover, the effect of addition of TMA to a MAO mixture has been examined.[8,9] However, the conclusions drawn from these studies are to some degree contradictory. Performing such a study successfully is a challenging task. Proton NMR gives a spectrum where the peaks from MAO and TMA overlap and the removal of volatiles produces more free TMA upon standing. Moreover, the usage of Lewis bases in such an analysis (in titration or as a probe molecule in heteronuclear NMR) is

(1) Zurek, E.; Woo, T. K.; Firman, T. K.; Ziegler, T. *Inorg. Chem.* **2001**, *40*, 361.
(2) Mason, M. R.; Smith, J. M.; Bott, S. G.; Barron, A. R. *J. Am. Chem. Soc.* **1993**, *115*, 4971.
(3) Pasynkiewicz, S. *Polyhedron* **1990**, *9*, 429.
(4) Tritto, I.; Sacchi, M. C.; Locatelli, P. *Macromol. Chem. Phys.* **1996**, *197*, 1537.
(5) Barron, A. R. *Organometallics* **1995**, *14*, 3581.
(6) Imhoff, D. W.; Simeral, L. S.; Samngokoys, S. Z.; Peel, J. H. *Organometallics* **1998**, *17*, 1941.
(7) Sinn, H. *Macromol. Symp.* **1995**, *97*, 27.
(8) Tritto, I.; Mealares, C.; Sacchi, M.; Locatelli, P. *Macromol. Chem. Phys.* **1997**, *198*, 3963.
(9) Eilertsen, J. L.; Rytter, E.; Ystenes, M. M. *Vib. Spectrosc.*, in press.

10.1021/ic001444z CCC: $20.00
Published on Web 05/31/2001

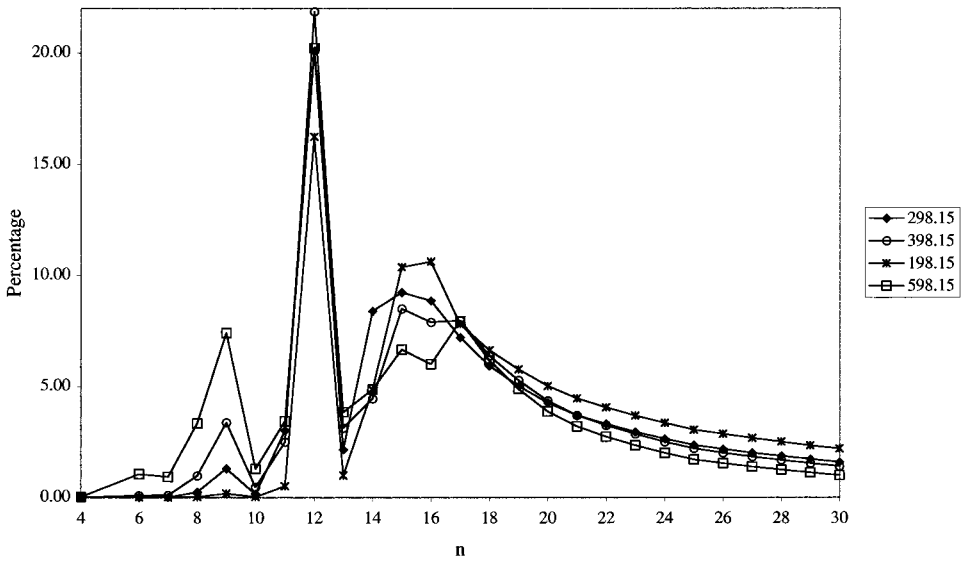

Figure 1. Composition of TMA Free $(AlOMe)_n$ as a Function of n within the Temperature Range of 198.15−598.15 K.

unreliable due to the fact that most bases not only interact with TMA, but also with MAO. Some experimental methods claim to have overcome these problems yielding a Me/Al ratio of 1.4[6] or 1.5[7] when free TMA has been removed or corrected for. This does not imply that structures containing this exact ratio may be found, but instead should be considered as a weighted average over all structures found within the MAO mixture.

Within this study we will expand upon the model which we have proposed for "pure MAO". [1] Here we will establish a percent abundance of different MAO species with the general formula $(AlOMe)_n \cdot (Al(CH)_3)_m$ where $4 \leq n \leq 30$ and $0 \leq m \leq 4$, depending upon the structural properties of the parent cage. Ultimately, it is the Gibbs free energy which determines the stability of a given structure. The Gibbs free energy is given as

$$G_T(n,m) = H_T(n,m) - TS_T(n,m) \qquad (2)$$

where $H_T(n,m)$ is the enthalpy at temperature T for $(AlOMe)_n \cdot (Al(CH)_3)_m$ and $S_T(n,m)$ is the corresponding entropy.

Section 3.1 discusses the different ways in which TMA may interact with MAO, showing that there is a certain preferred bonding mode. Section 3.2 examines the sites of greatest Latent Lewis Acidity on MAO cages where n ranges from 6 to 13. This is done by finding the bonds which give the most negative ΔE value when reacted with TMA. Sections 3.3, 3.4, and 3.5 discuss the energetic, enthalpic, and entropic contributions to the Gibbs free energy when 1−4 TMA groups are added to different MAO cages. In Section 3.6 the Gibbs Free Energy is used to find the percent abundance of each species within the temperature range of 198−598 K, and the ratio of Me/Al groups is calculated. Finally, in Section 3.7 the accuracy of the theoretical and experimental results is examined.

II. Computational Details

The density functional theory calculations were carried out using the Amsterdam Density Functional (ADF) program version 2.3.3 deverloped by Baerends et al.[10] and vectorized by Ravenek.[11] The numerical integration scheme applied was developed by te Velde et al.[12] and the geometry optimization procedure was based on the method of Verslius and Ziegler.[13] For total energies and geometry optimizations, the gradient corrected exchange functional of Becke[14] and the correlation functional of Perdew[15] were utilized in conjunction with the LDA parametrization of Vosko et al.[16] The electronic configurations of the molecular systems were described by a double-ζ STO basis set with one polarization function. A 1s frozen core was used for carbon and oxygen, while an [Ar] frozen core was used for aluminum. A set of auxiliary s, p, d, f, and g STO functions centered on all nuclei was used to fit the molecular density and represent Coulomb and exchange potentials in each SCF cycle.[17] Single-point numerical differentiation of energy gradients were used for frequency calculations.

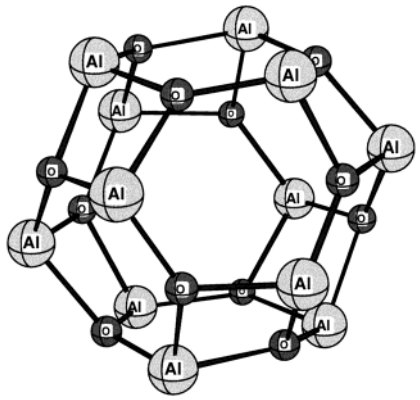

Figure 2. Most Stable MAO Cage at all Tempertures: $(AlOMe)_{12}$.

UFF2[18,19] was used to calculate entropic and finite temperature enthalpy corrections to the Gibbs free energy. Along with the parameters which have already been established previously[1] for four coordinate aluminum and oxygen, a new atom had to be introduced to represent three coordinate aluminum. The force field was reparametrized for this

(10) (a) Baerends, E. J.; Ellis, D. E.; Ros, P. *Chem. Phys.* **1973**, *2*, 41. (b) Baerends, E. J.; Ros, P. *Chem. Phys.* **1973**, *2*, 52.
(11) Ravenek, W. *Algorithms and Applications on Vector and Parallel Computers*; te Riele, H. J. J., Dekker: T. J., vand de Horst, H. A., Eds.; Elservier: Amsterdam, The Netherlands, 1987.
(12) (a) te Velde, G.; Baerends, E. J. *Comput. Chem.* **1992**, *99*, 84. (b) Boerringter, P. M.; te Velde, G.; Baerends, E. J. *Int. J. Quantum Chem.* **1998**, *33*, 87.
(13) Verslius, L.; Ziegler, T. *J. Chem. Phys.* **1988**, *88*, 322.
(14) Becke, A. D. *Phys. Rev. A* **1988**, *38*, 3098.
(15) Perdew, J. P. *Phys. Rev. B* **1986**, *33*, 8822.
(16) Vosko, S. H.; Wilk, L.; Nusaier, M. *Can. J. Phys.* **1980**, *58*, 1200.
(17) Krijn, J.; Baerends, E. J. *Fit Functions in the HFS-Method*; Free University of Amsterdam: Amsterdam, 1984.
(18) Casewit, A. K.; Colwell, K. S.; Rappe, A. K. *J. Am. Chem. Soc.* **1992**, *114*, 10046.
(19) Casewit, C. J.; Colwell, K. S.; Rappe, A. K.; *J. Am. Chem. Soc.* **1992**, *114*, 10035.

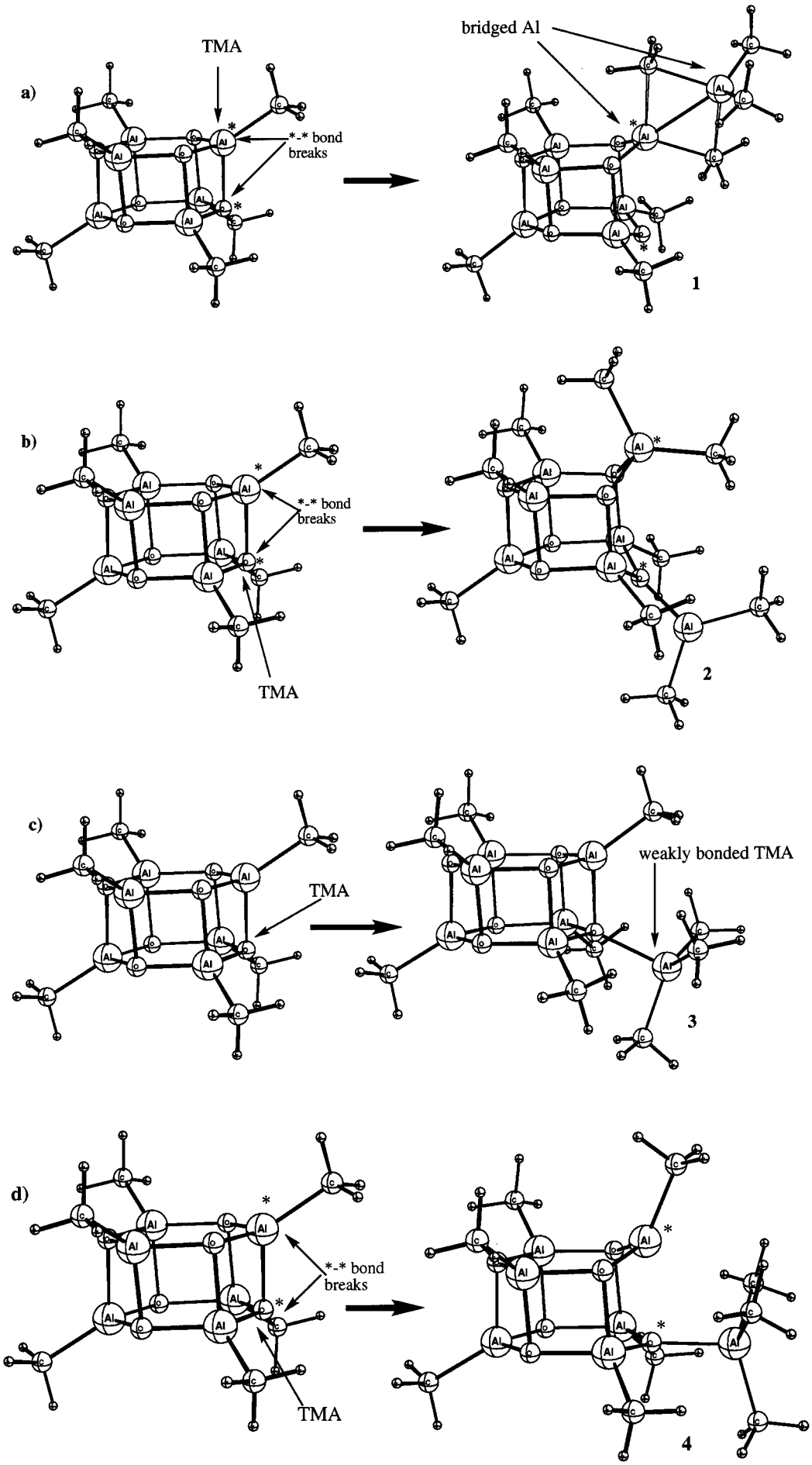
a)
TMA
- bond breaks
bridged Al
1
b)
- bond breaks
TMA
2
c)
TMA
weakly bonded TMA
3
d)
- bond breaks
TMA
4

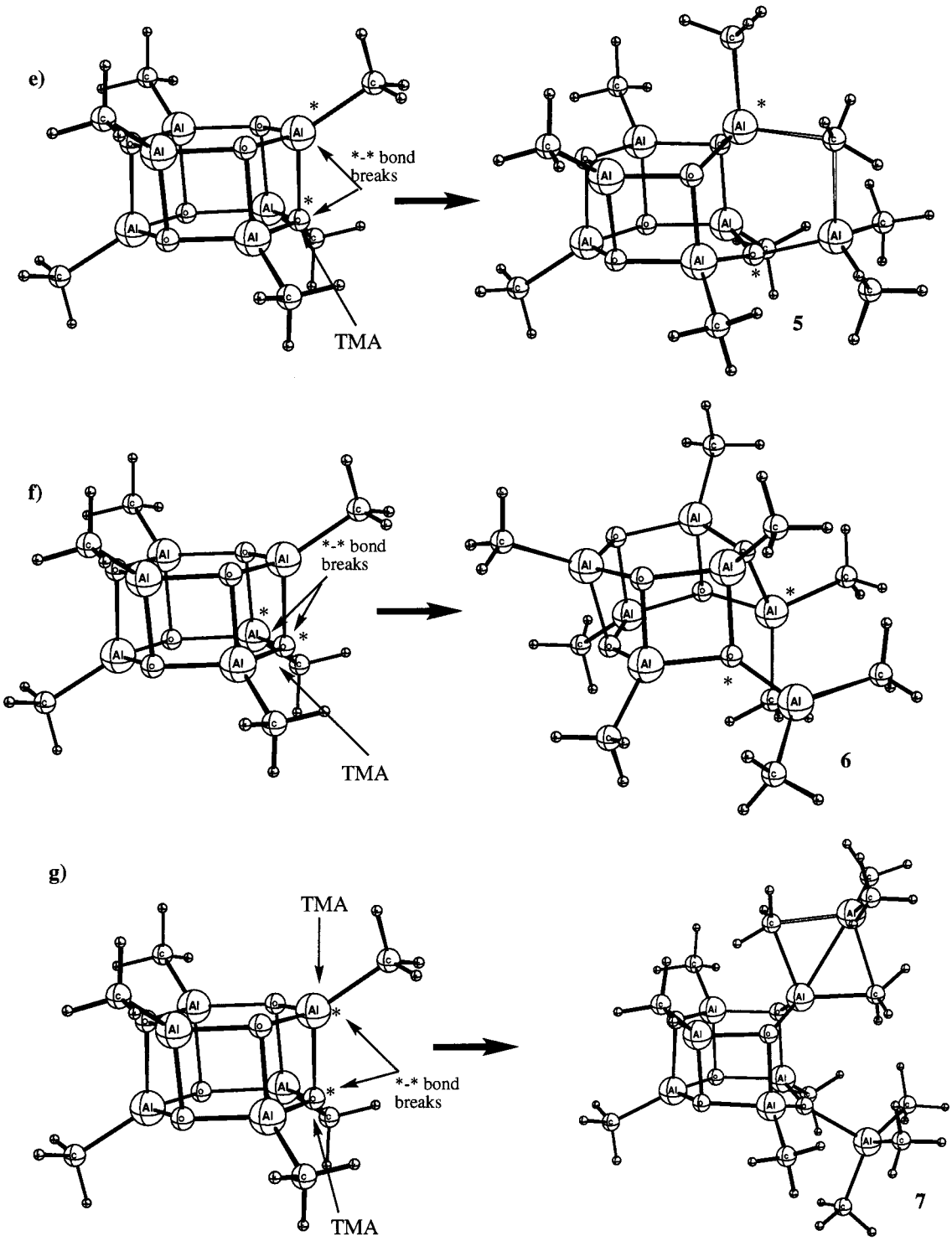

Figure 3. Possible Structures for $(AlOMe)_6 \cdot (TMA)$ and $(AlOMe)_6 \cdot (TMA)_2$.

new atom type. The original and reparametrized values are given in Tables 1.1−1.3 of Supporting Information.

Solvation calculations were done using the COSMO method[20a] as implemented in ADF.[20b] The solvent excluding surface was used along with an epsilon value of 2.379 for the solvent toluene. Atomic radii used were 2.3, 1.5, 2.0, and 1.16 Angstroms for Al, O, C, and H, respectively.

Structures and thermodynamic data for original MAO cage structures can be found elsewhere.[1] Here, we shall use and expand upon the methods and results established in our first paper on "pure" MAO.

(20) (a) Klamt, A.; Schuurmann, G. *J. Chem. Soc., Perkin. Trans. 2.* **1993**, 799. (b) Pye, C. C.; Ziegler, T. *Theor. Chem. Acc.* **1999**, *101*, 396.

III. Results and Discussion

3.1. How TMA Bonds with MAO. To determine the interaction of MAO and TMA, we must first of all examine how TMA bonds to MAO. Calculations have been performed on six different structural alternatives for the compound $(AlOMe)_6 \cdot (TMA)$. They are shown in Figure 3; the Cartesian coordinates are given in Table 2 of Supporting Information. The ΔE values for the reaction $^1/_2(TMA)_2 + (AlOMe)_6 \rightarrow (AlOMe)_6 \cdot (TMA)$ are given in Table 1, where E is the electronic contribution to the enthalpy. All energies are with respect to the TMA dimer, since this is the most likely species to exist in solution.

Scheme 1. Interaction of TMA with $(AlOMe)_6$.

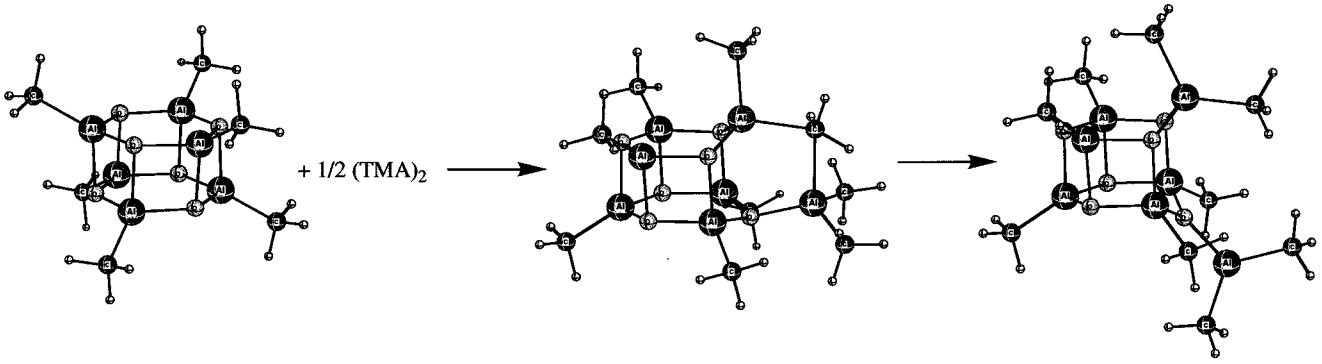

Table 1. ΔE for Reaction of $^1/_2(TMA)_2 + (AlOMe)_6$

structure	ΔE^a (kcal/mol)
1	14.89
2	−13.06
3	−1.01
4	6.26
5	−7.79
6	5.15

[a] E is the electronic contribution to the enthalpy.

In **1** the strained square−square (s−s) bond has broken and a TMA group has bonded to the corresponding Al atom via two bridging methyl groups. It is surprising to find that for this reaction ΔE is equal to 14.89 kcal/mol and hence this bonding mode is highly unfavorable. The strained s−s bond in **2** has also been broken. Yet, here the TMA has bonded to the O atom and a methyl transfer to the Al has occurred. This reaction has the lowest ΔE, and hence this is the preferred bonding mode. Structures **3** and **4** are quite similar in that the Al of the TMA is weakly bonded to the oxygen. In **3** the strained s−s bond is not broken, whereas in **4** it is. Neither structure is a favorable alternative. In **5** a s−s bond breaks and the Al of the TMA bonds to an O on the parent cage and to an Al via a methyl bridge. This reaction also has a negative ΔE value. Yet, it is not as low as in the case of **2**. In fact, **5** can be considered as the intermediate between $(AlOMe)_6 + {}^1/_2(TMA)_2$ and **2** as shown in Scheme 1. Other groups have proposed that TMA bonds to MAO in a manner analogous to that shown in **5**.[22] However, they did not perform explicit calculations on **2** to demonstrate that this is a more energetically favorable alternative. The exact same bonding has taken place in **6** as in **2**, yet the bond broken was a square-hexagonal (s−h) one. The ΔE here is positive showing that it is not only *how* TMA bonds to MAO, which is important, but also *where*. The s−s bond is much more strained than the s−h bond, thereby being much more acidic.

There is one other possibility which must be taken into consideration, that of structure **7**. Other groups have proposed that this is the preferred bonding mode of TMA.[23] Here we have two TMA groups bonding to the MAO cage simultaneously. However, our calculations show that ΔE is 4.02 kcal/mol for this reaction. Thus, it can be concluded that TMA bonds to MAO as shown in **2**. Structures with methyl bridges (**5**) and weak ion-pairs (**3**) ought to be present in the MAO mixture, but the completely ring-opened cages (**2**) show the predominant binding mode of TMA to MAO.

(21) Smith, M. B. *J. Organomet. Chem.* **1972**, *46*, 31.
(22) Ystenes, M.; Eilertsen, J. L.; Liu, J.; Ott, M.; Rytter, E.; Stovneng, J. A. *J. Polym. Sci. A* **2000**, *38*, 3106.

3.2. Sites of Greatest Latent Lewis Acidity Within Caged MAO Structures. TMA was added to $(AlOMe)_n$ cages, where $6 \le n \le 13$ consisting of square and hexagonal faces only, in a manner analogous to that shown in structure **2** above. Figure 4 displays only the sites which gave negative ΔE values for the reaction $^1/_2(TMA)_2 + (AlOMe)_n$. The Cartesian coordinates for the ring-opened compounds are given in Table 3 of Supporting Information. The site for $(AlOMe)_{12}$ is not shown in Figure 4, since the reaction gave a positive ΔE. The first thing which must be noted is that three variables are necessary in characterizing such sites. The first is what type of bond was broken (s−s, s−h, or h−h), the second and third correspond to the bonding environments of the O and Al atoms which comprised the broken bond. Here the bonding environments correspond to the types of faces that these atoms belonged to. Thus, in **2** above, the most acidic site had O and Al atoms in 2S + H environments and the bond that was broken was a s−s bond. Intuitively speaking, s−s bonds and atoms in 3S environments ought to experience higher ring strain thereby being most acidic. We shall now examine this in more detail.

Table 2 gives the ΔE values for the reaction at each particular site and Table 3 shows the three variables which are necessary to characterize the most acidic site for each $(AlOMe)_n$. In all cases but one the most Lewis acidic site corresponded to a s−s bond being broken with the corresponding Al in a 2S + H environment. Moreover, in each of the most acidic sites the O was in either a 2S + H or 3S environment. For $(AlOMe)_9$ the site which is most acidic is a s−h bond with an Al in a 2H + S environment and O in a 2S + H environment. The reason for it being more acidic than the s−s bond where both atoms belong to a 2S + H environment is likely due to the steric congestion present in the s−s bond opened product.

The above characterization suggests that $(AlOMe)_{12}$, the most stable $(AlOMe)_n$ cluster (see Figure 2), will not have any acidic sites, since all of the atoms belong to 2H + S environments. The bonds which can be found are s−h and h−h bonds. When TMA was added to a s−h bond (which ought to be more acidic than an h−h bond), ΔE was 1.70 kcal/mol. Hence, this reaction will not occur, agreeing with our prediction. In an earlier paper[1] we have shown that the most stable oligomers for $n \ge 14$ consist of atoms in 2H + S and 3H environments only. Thus, we can conclude that TMA will not react with $(AlOMe)_n$ where $n = 12$ and $n \ge 14$, due to the lack of strained bonds present in the most stable structural alternative.

3.3. Energetic Considerations. TMA was added to the sites which were determined as being acidic in $(AlOMe)_n$ where $6 \le n \le 13$ and $n \ne 12$. Depending upon the number of acidic bonds present in the parent cage, up to four TMA groups were added. We also took into account the different possible ways

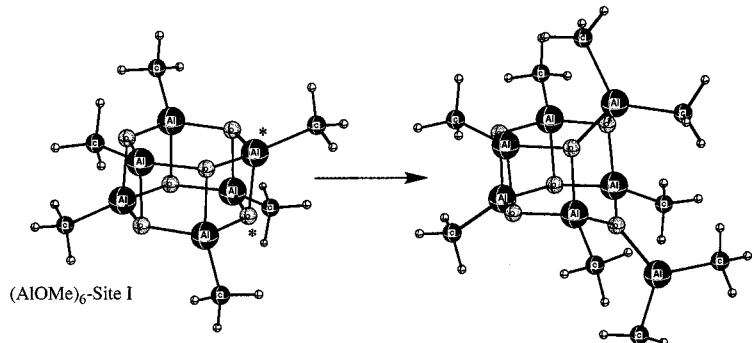

$(AlOMe)_6$-Site I

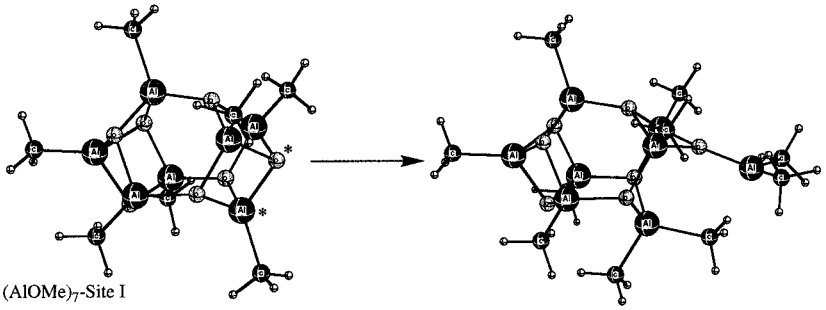

$(AlOMe)_7$-Site I

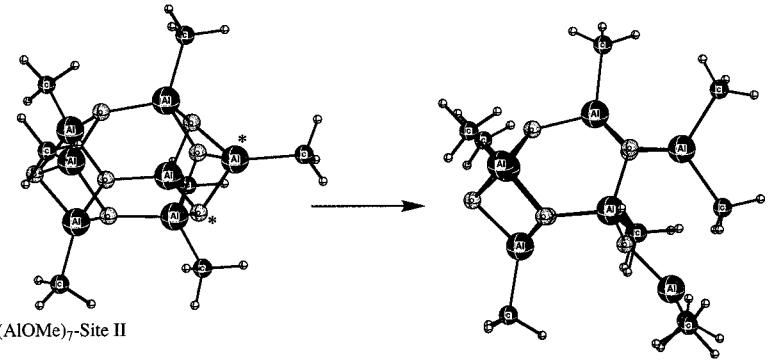

$(AlOMe)_7$-Site II

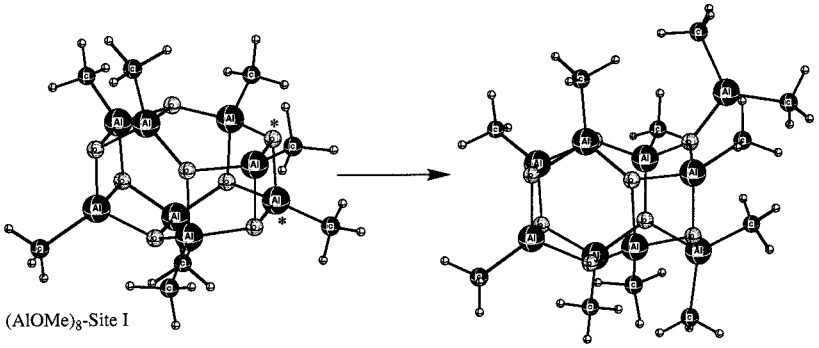

$(AlOMe)_8$-Site I

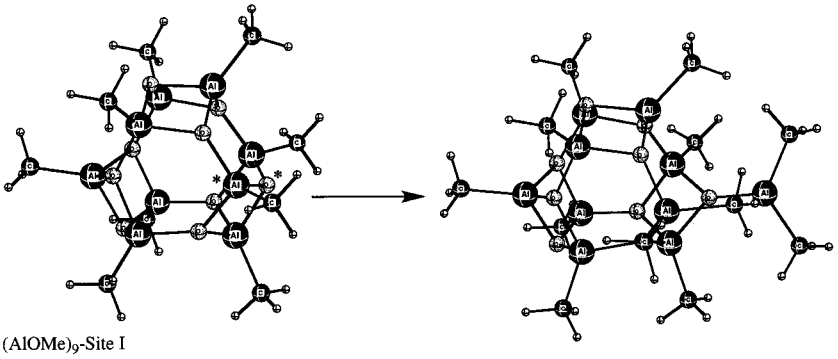

$(AlOMe)_9$-Site I

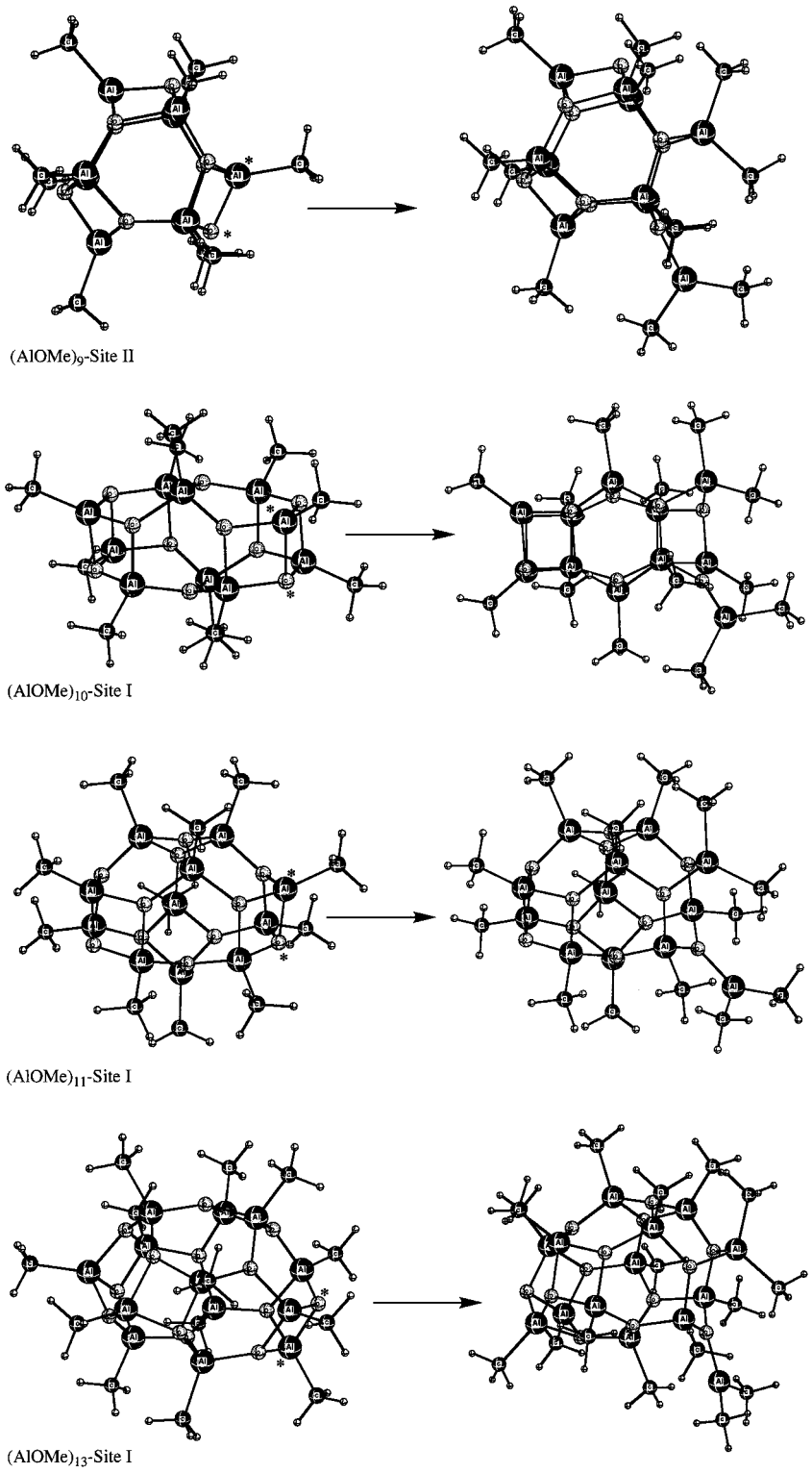

Figure 4. Acidic Bonds in $(AlOMe)_n$ cage structures where $6 \leq n \leq 13$ and $n \neq 12$.

TMA could be added. For example, in $(AlOMe)_7$ there are two types of acidic sites. Thus, one TMA could be added in two different ways. Moreover, due to the geometry of the parent cage, two TMAs could be added in two different ways. Not enough acidic sites are present to which a third TMA could be bonded in this case. In total, the geometry of 32 different $(AlOMe)_n \cdot (Al(CH)_3)_m$ structures was optimized. Their Cartesian coordinates are given in Table 4 of Supporting Information. In Figure 5 below, we give a graph of $\Delta E(n,m)$ corresponding to the number of TMA groups added. Only the values for the most stable structural alternatives are shown. For example, the addition of three TMA groups to $(AlOMe)_9$ can be done in four different ways with $\Delta E(n,m)$ ranging from between -3.87 kcal/mol to -9.23 kcal/mol. $\Delta E(n,m)$ the structure of lowest energy is given in Figure 5.

Figure 5 underlines that, for every MAO cage, the addition of TMA is energetically most favorable when two TMA groups are added. If the parent cage has more than two acidic sites

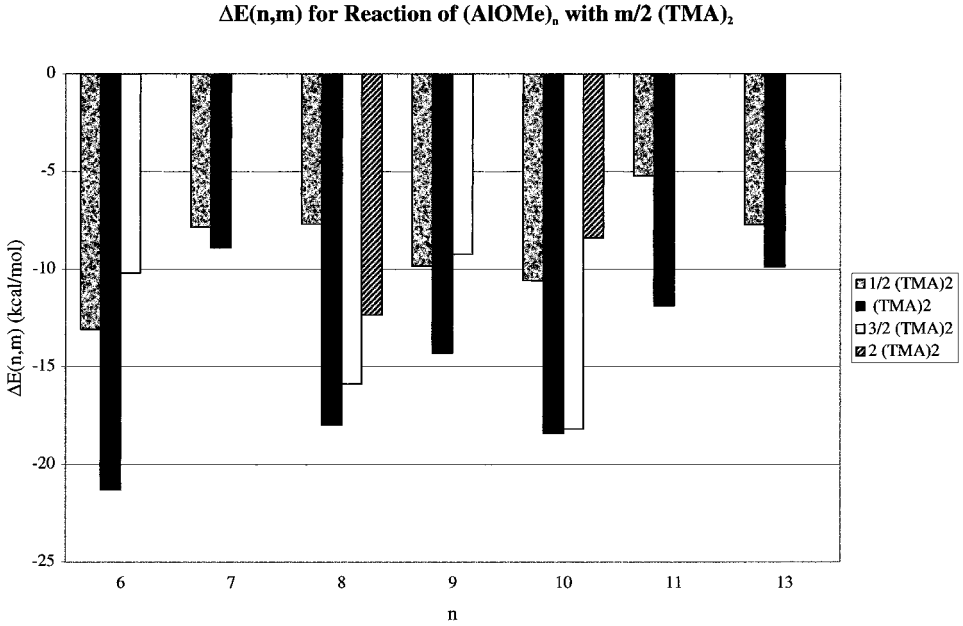

Figure 5. $\Delta E(n,m)$ for $(AlOMe)_n + {}^{m}/_{2}(TMA)_2 \rightarrow (AlOMe)_n{\cdot}(TMA)_m$.

Table 2. ΔE Values for the Reaction of $^{1}/_{2}(TMA)_2 + (AlOMe)_n$

n	site	ΔE (kcal/mol)
6	I	−13.06
7	I	−7.82
7	II	−4.73
8	I	−6.98
9	I	−9.82
9	II	−4.30
10	I	−10.56
11	I	−5.20
13	I	−7.70

Table 3. Variables Characterizing the Most Lewis Acidic Site for $(AlOMe)_n$

n	Al environment	O environment	bond broken
6	2S + H	2S + H	s−s
7	2S + H	3S	s−s
8	2S + H	2S + H	s−s
9	2H + S	2S + H	s−h
10	2S + H	2S + H	s−s
11	2S + H	2S + H	s−s
13	2S + H	2S + H	s−s

present and more than two TMA groups are added, steric repulsion becomes important and $\Delta E(n,m)$ for the addition of TMA becomes higher (less negative). Thus, energetically speaking, it is unfavorable to add more than two TMA groups to any MAO cage where $6 \leq n \leq 13$ and $n \neq 12$. If $n = 12$ or $n \geq 14$ then it is energetically unfavorable to add even one TMA group to the MAO cage.

Previously we have shown that structures which contained octagonal faces were less stable than those containing only square and hexagonal faces within the parent MAO cage. Yet here, we must take into account the possibility that when TMA reacts with these structures they become more stable than those where octagonal faces are not present. This could occur for two reasons. The first is that a greater amount of strain is present in these structures. Thus, when the strain is released $\Delta E(n,m)$ is low enough so that it decreases the energy of the ring-opened species to a value less than that of the ring-opened structures which contain no octagonal faces. The second is that the presence of octagonal faces introduces more acidic bonds with which TMA could react thereby lowering the energy of the structure sufficiently enough so that it is a viable alternative in solution.

We have explored the first option on two compounds. When comparing an $(AlOMe)_9$ structure containing one octagonal face which had been reacted with two TMA groups (in a manner which would introduce the least steric hindrance) to the *least* stable $(AlOMe)_9{\cdot}(TMA)_2$ structure whose parent cage had consisted of square and hexagonal faces only, we found that its energy was still greater by 20.22 kcal/mol. In the case of $(AlOMe)_8{\cdot}(TMA)_4$ composed of only square and hexagonal faces, quite a lot of steric hindrance is present. When considering the alternative structure containing two octagonal faces, much less steric hindrance exists. Yet, this structure has an energy which is still 6.45 kcal/mol higher.

The amount of acidic bonds present in the parent cage with which TMA may react is greatly dependent upon the geometry of the cage. For example, in $(AlOMe)_8$, up to four TMA groups could react with the cage, independent of whether it is one containing octagonal faces or not. For the case of $(AlOMe)_{11}$ only two TMA groups could be added to the cage not containing any octagonal faces whereas up to five TMA groups could be added to a structural alternative containing octagonal faces. However, such a ring opened structure should have quite a lot of steric hindrance, which we have seen increases the energy of the MAO·TMA compound despite the fact that ring strain in acidic bonds has been released. Moreover, entropically such a large structure would be unfavorable. Hence, within this study we decided to focus upon structures whose parent cages do not contain octagonal faces.

3.4. Enthalpic Considerations. Finite temperature enthalpies and entropies can be calculated from standard expressions[24] provided that all the vibrational frequencies are known (eqs 1−7 of Supporting Information). Unfortunately, fully quantum mechanical frequency calculations are computationally expensive and would require too much time to be performed on all

(23) Zakharov, I. I.; Zakharov, V. A.; Potaqpov, A. G.; Zhidomirov, G. M. *Macromol. Theory Simul.* **1999**, *8*, 272.
(24) Hehre, W. J.; Radom, L.; Schleyer, P. I. R.; Pople, J. A. *Ab Initio Molecular Orbital Theory*; John Wiley & Sons: New York, 1986.

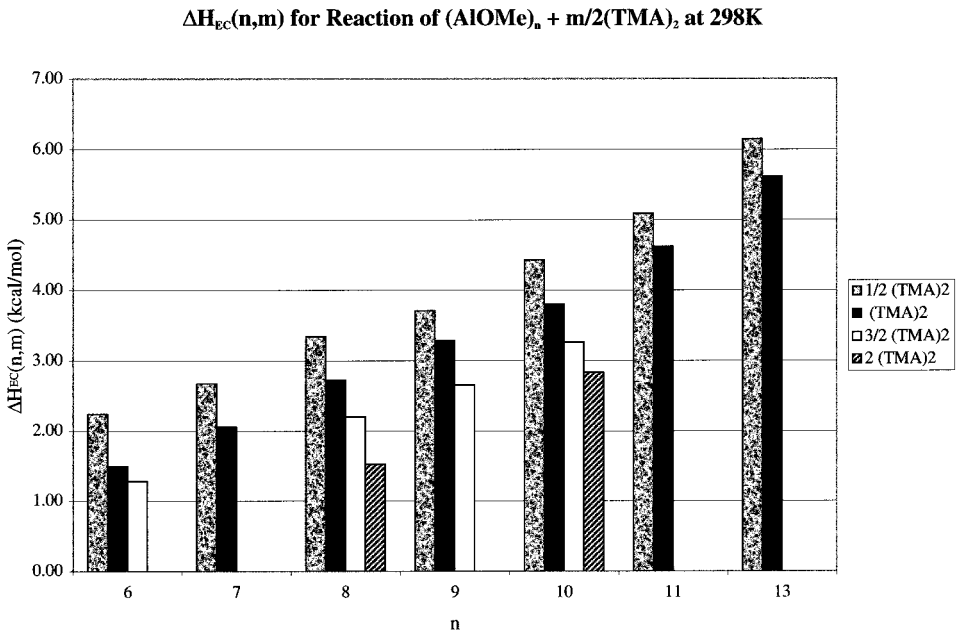

Figure 6. $\Delta H_{EC}(n,m)$ for $(AlOMe)_n + {}^{m}/_{2}(TMA)_2 \rightarrow (AlOMe)_n{\cdot}(TMA)_m$ at 298.15 K.

Table 4. Comparison of Thermodynamic Properties Obtained Using UFF2 and ADF

structure	ADF H_{EC}	UFF H_{EC}	ADF entropy	UFF entropy
$(AlOMe)_6{\cdot}TMA)_1$	235.12	236.39	216.27	210.20
$(AlOMe)_6{\cdot}(TMA)_2$	306.31	305.73	262.77	253.88
$(AlOMe)_8{\cdot}(TMA)_1$	291.57	293.93	255.88	248.70

* H_{EC}'s given in kcal/mol; Entropies in cal/molK at 298.15 K.

structures. Thus, another approach was taken, based on molecular mechanics calculations using the Universal Force Field.[18,19] First it was necessary to parametrize UFF2 so that the frequencies calculated agreed with those of ADF.

The original and optimized parameters of UFF2 are given in Tables 1.1−1.3 of Supporting Information. The results of the ADF and UFF2 calculations for the finite temperature enthalpy corrections (H_{EC}) and entropies at 298.15 K are given in Table 4. The parametrization was performed on $(AlOMe)_6{\cdot}(TMA)_1$ and checked on $(AlOMe)_6{\cdot}(TMA)_2$ and $(AlOMe)_8{\cdot}(TMA)_1$.

UFF2 estimates differ from values calculated by ADF for the finite temperature enthalpy correction by 1.27, −0.58, and 2.36 kcal/mol and underestimate the entropy by −1.81, −2.65, and −2.14 kcal/mol for $(AlOMe)_6{\cdot}(TMA)_1$, $(AlOMe)_6{\cdot}(TMA)_2$, and $(AlOMe)_8{\cdot}(TMA)_1$, respectively, at 298.15 K. These deviations are reasonable and represent an error of a few percent (percent error is less than 1% in all of the above calculations). Moreover, we have shown that the error does not increase when more than one TMA group is added to the parent cage. In fact, in this particular case the error is lower for $(AlOMe)_6{\cdot}(TMA)_2$ than for $(AlOMe)_8{\cdot}(TMA)_1$.

We can also consider the error in $\Delta H_{EC}(n,m)$ (defined in eq 3c below) and in $-T\Delta S(n,m)$ (defined in eq 4b below). They are 1.26, −0.582, and 2.32 kcal/mol for the former and 0.85, 1.70, and 2.64 kcal/mol for the latter for the formation of $(AlOMe)_6{\cdot}(TMA)_1$, $(AlOMe)_6{\cdot}(TMA)_2$, and $(AlOMe)_8{\cdot}(TMA)_1$, respectively, at 298.15 K. Thus for $\Delta G(n,m)$ the difference between the ADF and UFF values should be within 5 kcal/mol.

The total enthalpy is given as

$$H_T(n,m) = E(n,m) + H_{EC}(n,m) \qquad (3a)$$

where $E(n,m)$ is the electronic contribution to the enthalpy for $(AlOMe)_n{\cdot}(TMA)_m$ and $H_{EC}(n,m)$, the finite temperature enthalpy correction at temperature T is given by

$$H_{EC}(n,m)_{(T)} = H_{rot(T)} + H_{trans(T)} + H_{vib(T)} \qquad (3b)$$

Here $H_{rot(T)}$, $H_{trans(T)}$, and $H_{vib(T)}$ are the rotational, translational, and vibrational finite temperature enthalpy corrections at temperature T, respectively. Note that when $T = 0$ the zero-point energy is obtained.

Figure 6 shows the difference in the finite temperature enthalpy correction

$$\Delta H_{EC}(n,m) = H_{EC}(n,m) - H_{EC}((AlOMe)_n) - H_{EC}\left(\frac{m}{2}(TMA)_2\right) \qquad (3c)$$

for the reaction in eq 1. It is given as a function of n, when one, two, three, and four TMA groups are added to the parent cage at 298.15 K. It can be noted that $\Delta H_{EC}(n,m)$ increases with increasing n value within a given series (how many TMAs are added). In fact, the increase follows a linear relationship. Thus, for one TMA added $\Delta H_{EC}(n,1) = 0.569n - 1.254$ kcal/mol with an rms deviation of 0.08 kcal/mol. For two TMAs added $\Delta H_{EC}(n,2) = 0.597n - 2.095$ kcal/mol with an rms deviation of 0.07 kcal/mol. For three and four TMAs added no linear regression was performed due to the lack of data points present.

It must also be noted that as the number of TMA's added increases the $\Delta H_{EC}(n,m)$ value decreases for a given n. From the few data points available, this also appears to follow a linear relationship. Moreover, $\Delta H_{EC}(n,m)$ increases with increasing temperature. For the reaction $(AlOMe)_6 + {}^{1}/_{2}(TMA)_2 \rightarrow (AlOMe)_6{\cdot}(TMA)_1$ it is 1.64, 2.24, 2.74, and 3.57 kcal/mol for 198, 298, 398, and 598 K, respectively. At different temperatures, the same aforementioned relationships for $\Delta H_{EC}(n,m)$ holds.

Table 5a−d of Supporting Information lists the energies, finite temperature enthalpy corrections, entropies, Gibbs free energies, and percent abundance in the temperature range of 198−598 K

Table 5. Percent Abundance of $(AlOMe)_n \cdot (TMA)_m$ at Different Temperatures

n	*m*	198.15 K	298.15 K	398.15 K	598.15 K
6	0	0.00	0.01	0.07	0.86
6	1	0.00	0.02	0.15	0.84
6	2	0.00	0.04	0.15	0.46
6	3	0.00	0.00	0.00	0.02
7	0	0.00	0.01	0.08	0.76
7	1	0.00	0.00	0.04	0.31
7	2	0.00	0.00	0.00	0.07
8	0	0.01	0.22	0.83	2.74
8	1	0.01	0.12	0.36	0.95
8	2	0.17	0.60	1.05	1.73
8	3	0.02	0.07	0.13	0.22
8	4	0.00	0.02	0.04	0.08
9	0	0.17	1.22	2.91	6.03
9	1	0.26	1.12	2.18	3.75
9	2	0.35	0.92	1.44	2.08
9	3	0.05	0.18	0.36	0.61
10	0	0.01	0.13	0.39	1.04
10	1	0.02	0.12	0.28	0.58
10	2	0.12	0.39	0.70	1.14
10	3	0.03	0.09	0.14	0.21
10	4	0.00	0.01	0.02	0.05
11	0	0.47	2.36	2.15	2.81
11	1	0.20	0.63	1.01	1.42
11	2	0.32	0.54	0.65	0.71
12	0	15.27	19.05	18.92	16.56
13	0	0.91	2.02	2.70	3.13
13	1	0.42	0.81	1.02	1.13
13	2	0.29	0.45	0.52	0.53
14	0	8.30	7.90	6.88	5.23
15	0	9.67	8.77	7.33	5.45
16	0	9.92	8.33	6.88	4.89
17	0	7.31	6.80	6.88	6.51
18	0	6.28	5.56	5.55	5.06
19	0	5.46	4.73	4.56	3.99
20	0	4.75	4.03	3.75	3.16
21	0	4.18	3.46	3.22	2.62
22	0	3.80	3.09	2.82	2.24
23	0	3.46	2.76	2.47	1.91
24	0	3.14	2.46	2.17	1.63
25	0	2.86	2.20	1.90	1.40
26	0	2.67	2.03	1.73	1.25
27	0	2.50	1.88	1.58	1.12
28	0	2.34	1.74	1.44	1.01
29	0	2.19	1.61	1.32	0.90
30	0	2.05	1.49	1.20	0.81

for all of the species whose Cartesian coordinates are given in Table 4 of Supporting Information.

3.5. Entropic Considerations. Entropic values were calculated via the parametrized UFF2 code. The total entropy of $(AlOMe)_n \cdot (TMA)_m$ at temperature T is given by

$$S_T(n,m) = S_{trans} + S_{rot} + S_{vib} \quad (4a)$$

where S_{trans}, S_{rot}, and S_{vib} are the translational, rotational, and vibrational contributions to the entropy. It is interesting to examine the contribution to the free energy of reaction $\Delta G(n,m)$ for the process in eq 1 due to the entropy change at a given temperature, $-T\Delta S(n,m)$ defined in eq 4b below.

$$-T\Delta S(n,m) = -\left(TS(n,m) - TS((AlOMe)_n) - TS\left(\frac{m}{2}(TMA)_2\right)\right) \quad (4b)$$

This is shown in Figure 7 for the most stable structure for a given n and m. $-T\Delta S(n,1)$ varies between 6.54 and 8.69 kcal/mol with an average value of 7.77 kcal/mol. Thus, in order for such a reaction to be favorable, the enthalpy must be at least −7.77 kcal/mol. $-T\Delta S(n,2)$ varies between 12.73 and 16.85 kcal/mol, with an average value of 7.50 kcal $mol^{-1}m^{-1}$; $-T\Delta S(n,3)$ varies between 17.23 and 21.48 kcal/mol with an average value of 6.50 kcal $mol^{-1}m^{-1}$ and for $-T\Delta S(n,4)$ the average is 5.43 kcal $mol^{-1}m^{-1}$. Thus the contribution from $-T\Delta S(n,m)$ per TMA unit decreases for every TMA being added.

In general $-T\Delta S(n,m)$ increases at higher temperatures. For example, for the reaction $(AlOMe)_9 + (TMA)_2 \rightarrow (AlOMe)_9 \cdot (TMA)_2$, $-T\Delta S(9,2)$ is 11.24, 15.71, 20.01, and 28.43 kcal/mol at 198, 298, 398, and 598 K, respectively. This is due to the fact that at higher temperatures smaller structures are more stable due to entropic effects. Thus, in the aforementioned reaction, the left-hand side of the equation will be more favorable at higher temperatures.

3.6. The Gibbs Free Energy and Percent Abundance. The Gibbs free energy has already been defined in eq 2. The free energy change $\Delta G(n,m)$ for the reaction given in eq 1 is plotted for the most stable structural alternatives in Figures 8a−8d at 198, 298, 398, and 598 K, respectively. At 298 K there are only four reactions with negative $\Delta G(n,m)$ values. They are for the addition of one and two TMA groups to $(AlOMe)_6$ and the addition of two TMA groups to $(AlOMe)_8$ and $(AlOMe)_{10}$. However, it must be noted that these $\Delta G(n,m)$ values are quite small. This indicates that not many $(AlOMe)_n \cdot (TMA)_m$ species will be present in MAO. Moreover, taking into account the fact that the abundance of the parent cages in "pure MAO" was calculated as being quite low (0.01%, 0.23%, and 0.14%, respectively, see Figure 1); this shows quite clearly that at 298 K very little TMA is bound to the MAO cages.

As the temperature increases and entropic effects become more important in destabilizing larger compounds, even fewer $\Delta G(n,m)$ values are negative. At 398 K the only negative values occur when one and two TMA groups are added to $(AlOMe)_6$, while at 598 K no negative values occur. However, small MAO cages are stabilized at higher temperatures (see Figure 1). Thus, despite the fact that few, if any, negative $\Delta G(n,m)$ values are present, since the parent cage has a higher percent abundance, more TMA will be bound to MAO at higher temperatures. At lower temperatures the opposite occurs. Hence at 198 K, there are 10 reactions with negative $\Delta G(n,m)$ values. However, entropic effects also tend to stabilize the large MAO cages. Thus, when only "pure MAO" is taken into consideration the percent abundance is 0%, 0%, 0.01%, 0.18%, and 0.01% for $n = 6$, 7, 8, 9, and 10, respectively (see Figure 1). Since the parent cages are not in high abundance neither will be the corresponding $(AlOMe)_n \cdot (TMA)_m$ species despite the fact that the Gibbs free energy for the reaction is negative. Thus, even in this case not much TMA is predicted to be bound to MAO.

The change in Gibbs free energy for the process in eq 5 is given in eq 6a.

$$n(AlOMe) + \frac{m}{2}(TMA)_2 \rightarrow (AlOMe)_n \cdot (TMA)_m \quad (5)$$

$$\frac{\Delta G_0(n,m)}{n} = \frac{G^0_T(n,m)}{n} - G^0_{T(AlOMe)} - \frac{m}{2n}G^0_{T(TMA)_2} \quad (6)$$

Defining $\Delta G_0(n,m)$ as in 6 it is then possible to calculate the equilibrium constant for the process given in eq 5 via eq 7.

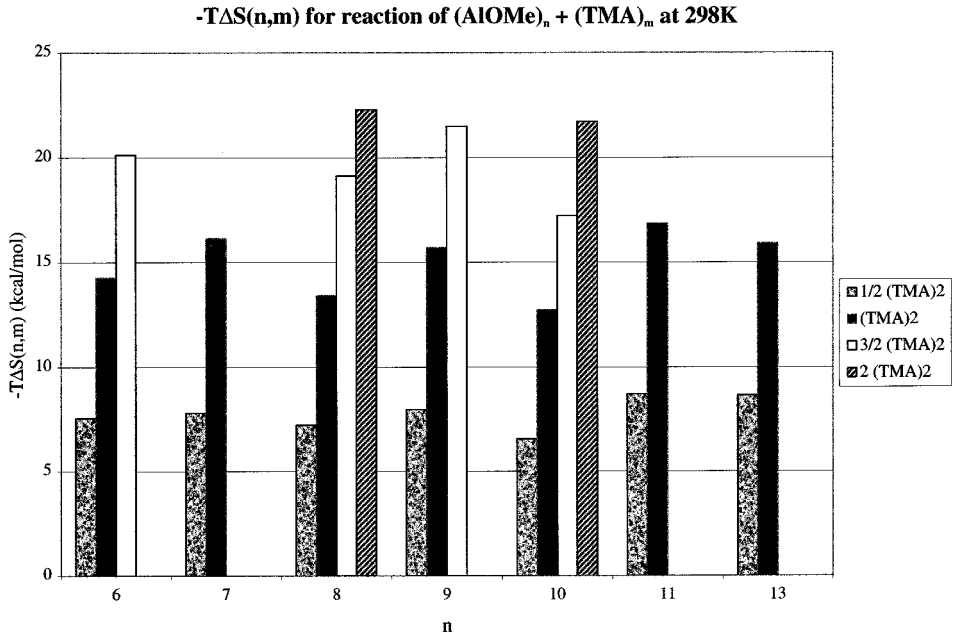

Figure 7. $-T\Delta S(n,m)$ for $(AlOMe)_n + {}^m/_2(TMA)_2 \rightarrow (AlOMe)_n\cdot(TMA)_m$ at 298.15 K.

Table 6. Analysis of the Amount of Bound TMA Present in a MAO Solution

temp (K)	Me/Al	Al_{TMA}/Al_{tot} (%)
198.15	1.00	0.21
298.15	1.01	0.62
398.15	1.02	1.05
598.15	1.03	1.76

Next, the percent abundance of a given structure may be found according to eq 8.

$$K_{eq}(n,m) = \exp(-\Delta G_0(n,m)/nRT) \quad (7)$$

$$\%(AlOMe)_n(TMA)_m = \{(K_{eq}(n,m) \times [(TMA)_2]^{m/2n})/ \sum_m\sum_n (K_{eq}(n,m) \times [(TMA)_2]^{m/2n})\} \times 100\% \quad (8)$$

The percent abundance of the possible $(AlOMe)_n\cdot(TMA)_m$ structures was found at 198, 298, 398, and 598 K and is given in Table 5. It is dependent upon the concentration of TMA found in the solution. The numbers given in the table are a sum of the percentage of all possible isomers considered for a given $(AlOMe)_n\cdot(TMA)_m$ for 1 mol/L TMA. Percents for individual isomers are given in Supporting Information Figures 5a−d. Changing the TMA concentration has little effect on the overall Me/Al ratio. For small concentrations $[(TMA)_2]^{m/2n}$ approaches 0 and the ratio goes to 1, whereas for concentrations within the range of 1−20 mol/L, $[(TMA)_2]^{m/2n}$ is approximately equal to 1. Even at concentrations of 100 mol/L, at 398.15 K the Me/Al ratio increases to 1.03 from 1.02. Hence, despite the fact that increasing the concentration of TMA changes the percentages of individual components slightly, the overall Me/Al ratio remains virtually unchanged. Table 6 gives the Me to Al ratio as well as the percent of Al found as bound TMA of the total aluminum content in MAO (free TMA is neglected) at 1 mol/L TMA. This ratio is more sensitive to the change of TMA concentration than is the total Me/Al ratio. For example, it increases to 1.33 at a TMA concentration of 20 mol/L at 398.15 K.

Our results lead to the conclusion that very little TMA is bound to MAO within the temperature range of 198.15−598.15 K. Most TMA exists as the dimer in solution. Higher temperatures somewhat facilitate the binding of TMA to MAO, but only very slightly. The percent of Al which exist as TMA (of the total Al content) increases by 1.55% throughout a temperature range of 400 K. The CH_3 to Al ratio found is ∼1 at all temperatures and does not agree with experimental data which suggests a number near 1.5. We shall comment on this discrepancy in the next section.

Table 7. The Effect of Changing $\Delta G(n,m)$, Where $m = 2$, on the Me/Al Ratio in MAO for the Reaction $(AlOMe)_n + {}^m/_2(Al(CH_3)_3)_2 \leftrightarrow (AlOMe)\cdot(Al(CH_3)_3)_m$ at 298.15 K

$\Delta G(n,2)$ (kcal/mol)	Me/Al
10	1.00
−10	1.06
−15	1.14
−20	1.27
−25	1.39
−30	1.47

3.7. Analysis of Theoretical and Experimental Results. We shall now turn toward a discussion of possible sources of error in the experimental and theoretical procedures used to determine the bound TMA content in MAO.

Errors in the Calculations. We have calculated the free energy of dimerization for TMA as being $\Delta G_d^0 = 0.38$ kcal/mol at 298 K. This value is larger than the experimental estimate[21] of −7.46 kcal/mol. We note that the deviation is larger than the standard error of ±5 kcal/mol associated with our DFT calculations. The first thing which must be done to determine if the discrepancy between theory and experiment is due to errors in the calculated numbers is to determine how much the numbers must change for the Me/Al ratio to increase to 1.5.

Table 7 shows how changing $\Delta G(n,2)$ for the process shown in **1** influences the Me/Al ratio at 298 K. A negative number for $\Delta G(n,2)$ denotes lowering the calculated $\Delta G(n,2)$ by that amount; a positive number raising it. In light of the error present in the Gibbs free energy of dimerization, it is reasonable to assume that the $\Delta G(n,m)$ values for the process shown in eq 1 are good to within ±10 kcal/mol for each dimer of TMA present in the reaction. Table 7 shows that decreasing $\Delta G(n,2)$ by 10 kcal/mol raises the Me/Al ratio to 1.06 and increasing it by 10 kcal/mol lowers it to 1.00. To achieve the experimental ratio, $\Delta G(n,m)$ would have to be decreased by 32 kcal/mol for each

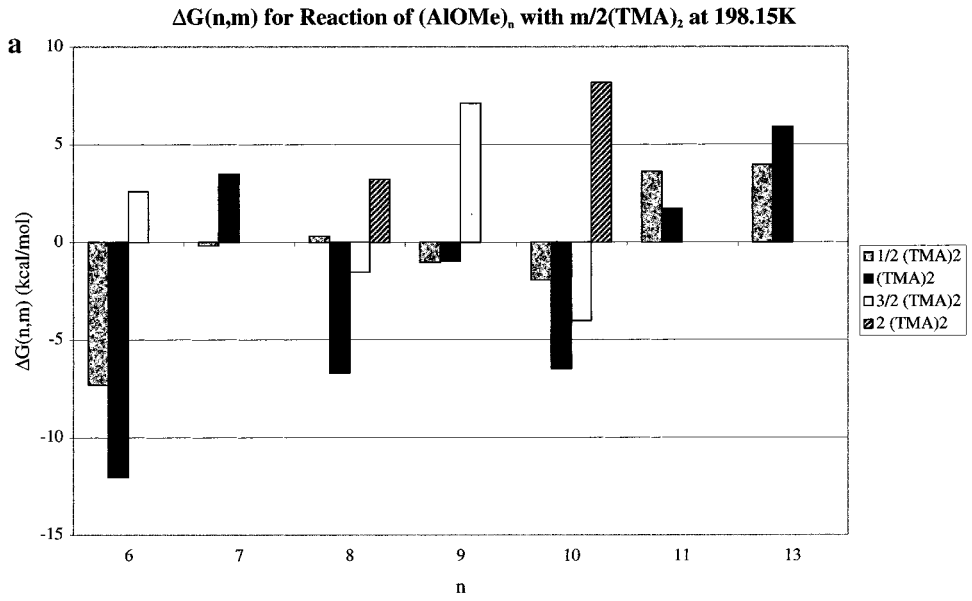
a
ΔG(n,m) for Reaction of (AlOMe)n with m/2(TMA)2 at 198.15K
ΔG(n,m) (kcal/mol)
10
5
0
-5
-10
-15
6
7
8
9
10
11
13
n
1/2 (TMA)2
(TMA)2
3/2 (TMA)2
2 (TMA)2

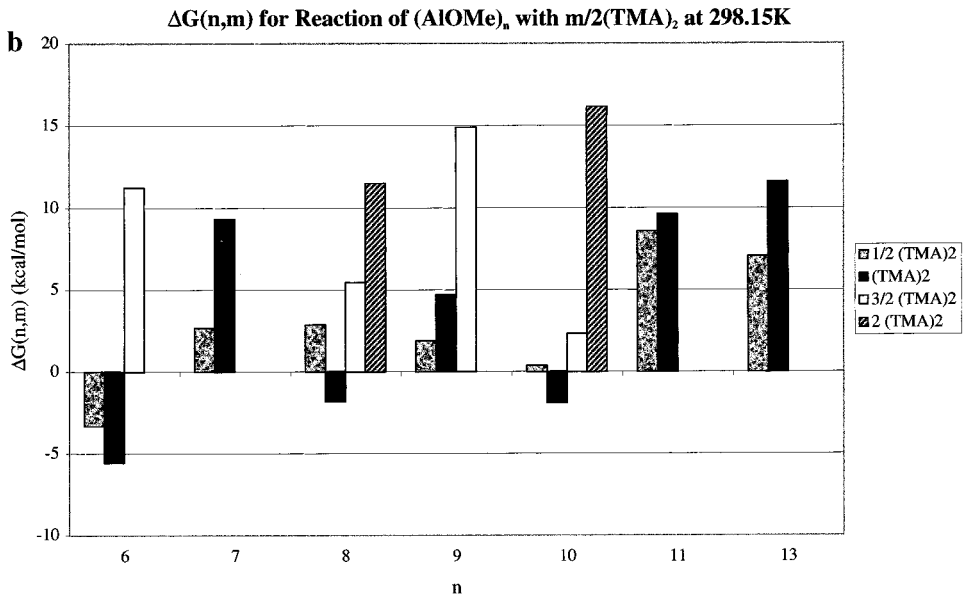
b
ΔG(n,m) for Reaction of (AlOMe)n with m/2(TMA)2 at 298.15K
ΔG(n,m) (kcal/mol)
20
15
10
5
0
-5
-10
6
7
8
9
10
11
13
n
1/2 (TMA)2
(TMA)2
3/2 (TMA)2
2 (TMA)2

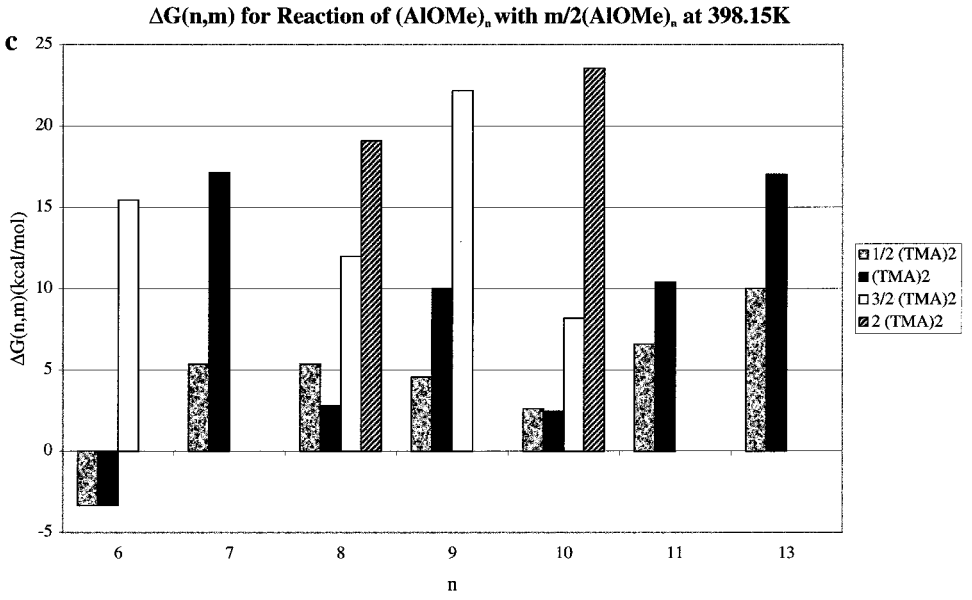
c
ΔG(n,m) for Reaction of (AlOMe)n with m/2(AlOMe)n at 398.15K
ΔG(n,m)(kcal/mol)
25
20
15
10
5
0
-5
6
7
8
9
10
11
13
n
1/2 (TMA)2
(TMA)2
3/2 (TMA)2
2 (TMA)2

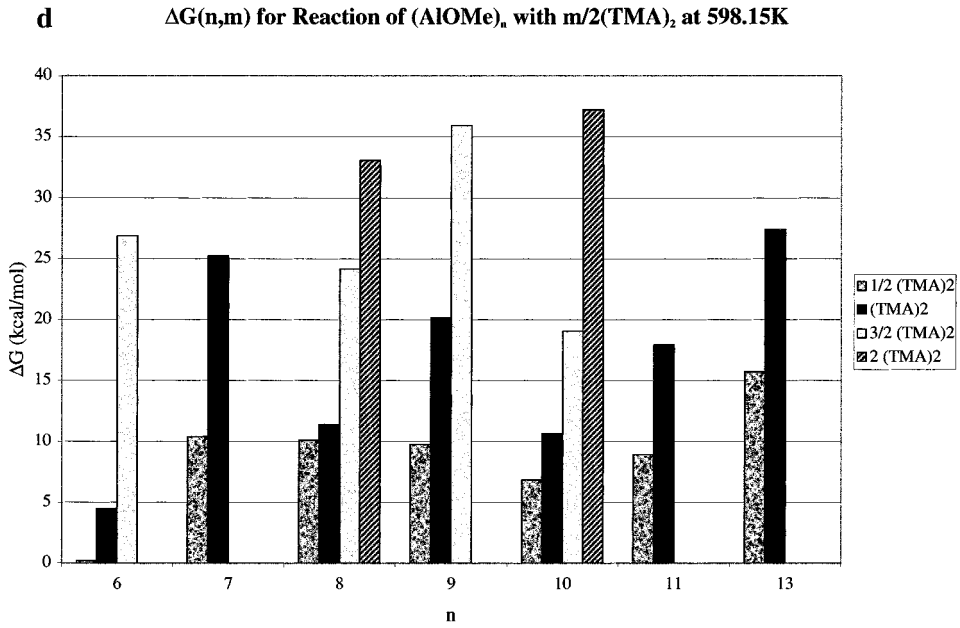

Figure 8. $\Delta G(n,m)$ for $(AlOMe)_n + {}^{m}/_{2}(TMA)_2 \rightarrow (AlOMe)_n{\cdot}(TMA)_m$ at a) 198.15 K b) 298.15 K c) 398.15 K d) 598.15 K.

TMA dimer present in the reaction. It is highly improbable that errors of this magnitude would be present in an ADF calculation.

Solvent Effects. MAO solutions are often made by the controlled hydrolysis of TMA in toluene or other hydrocarbon solvent. Moreover, it can be quite difficult to remove all of the solvent from the MAO solution.[7] Thus, we decided to examine if the inclusion of solvent effects had much of an impact on the calculated results. Solvent parameters for toluene were used. The inclusion of solvent effects for the reaction shown in **9**increased $\Delta E(6,1)$ by 0.76 kcal/mol in comparison to the gas-phase value. This shows that solvent effects are negligible.

$$(AlOMe)_6 + \frac{1}{2}(TMA)_2 \rightarrow (AlOMe)_6{\cdot}(TMA) \qquad (9)$$

Other Possible Bonding Modes. We have studied six possible bonding modes of a single molecule of TMA to a MAO cage. To our knowledge, there are no other possible ways in which this may be done. We have also studied one possible bonding mode of two TMA groups to a single MAO cage (structure **7**), showing that this is not a favorable bonding alternative. Despite the fact that there may exist other ways in which two or more TMA groups can bind to a single MAO cage, it seems unlikely that these will be more stable alternatives to the bonding mode shown in structure **2**.

Analysis of Experimental Data and Techniques. Simeral and co-workers developed a technique to determine the amount of bound and free TMA in a MAO solution using proton NMR.[6] They found the addition of tetrahydrofuran (THF) to MAO resulted in the downfield movement of the peak attributed to TMA and only a slight downfield movement of the MAO. In such a manner, the two peaks became nearly resolved. They attributed this to the formation of an adduct between the THF and TMA. Next, curve fitting was used to resolve the two peaks. It was then possible to determine the amount of H groups, and hence CH_3 groups, which belong to TMA and those to MAO. Total Al content was determined via wet chemical methods and ICP-AE (inductively coupled plasma atomic emission). Knowing total Al, total TMA, and the amount of Me present in MAO, it is then possible to determine the Me/Al ratio. They determined this ratio as being 1.4−1.5.

The validity of this method relies on the assumption that THF does not facilitate the bonding of TMA groups to MAO. However, we have shown that the assumption is invalid. Figure 9 shows a number of possible reactions which could occur when THF is added to MAO along with the energy change for the reaction. Reaction 1 corresponds to the formation of an adduct between THF and free TMA. The energy change is −14.17 kcal/mol underlining that this does indeed occur. Reaction 2 has a ΔE value of only −6.56 kcal/mol demonstrating that THF hardly binds to MAO. In reaction 3, the O of the THF bonds to an Al on the MAO. Moreover, an Al from a free TMA group bonds to an O on the MAO. A strained square−square bond is broken in the process. This reaction has a ΔE value of −23.15 kcal/mol. This clearly indicates that when THF is added to MAO not only is an adduct formed. Moreover, the THF facilitates the bonding of a TMA group to a MAO cage thereby inflating the Me/Al ratio. This result also shows us that the presence of basic impurities in the MAO mixture can increase the amount of TMA which is bound to the $(AlOMe)_n$ cages. Moreover, it may lead to the formation of MAOs with a smaller average *n* value.

Decomposition of $(AlOMe)_n$. It has been shown experimentally that a MAO solution from which TMA has been removed develops more free TMA upon standing.[5] This has been attributed to the equilibrium shown in eq 1 shifting to the left. Our calculations show that there is very little TMA bound to MAO, thus we propose that $(AlOMe)_n$ undergoes a slow decomposition which results in the formation of aluminoxane and TMA dimer. This can be seen most clearly in eq 10. Upon removal of TMA the equilibrium shifts to the right and more free TMA is observed.

$$(AlOMe)_n \leftrightarrow Al_{(n-2)}O_nMe_{(n-6)} + (TMA)_2 \qquad (10)$$

IV. Conclusions

Within this study we have proposed a model for TMA containing MAO. We have first of all found that TMA bonds to MAO via breaking a strained acidic bond. An $AlMe_2$ group attaches to an O of the cage and a Me is transferred to the corresponding Al. The acidic sites for *n* ranging between 6 and

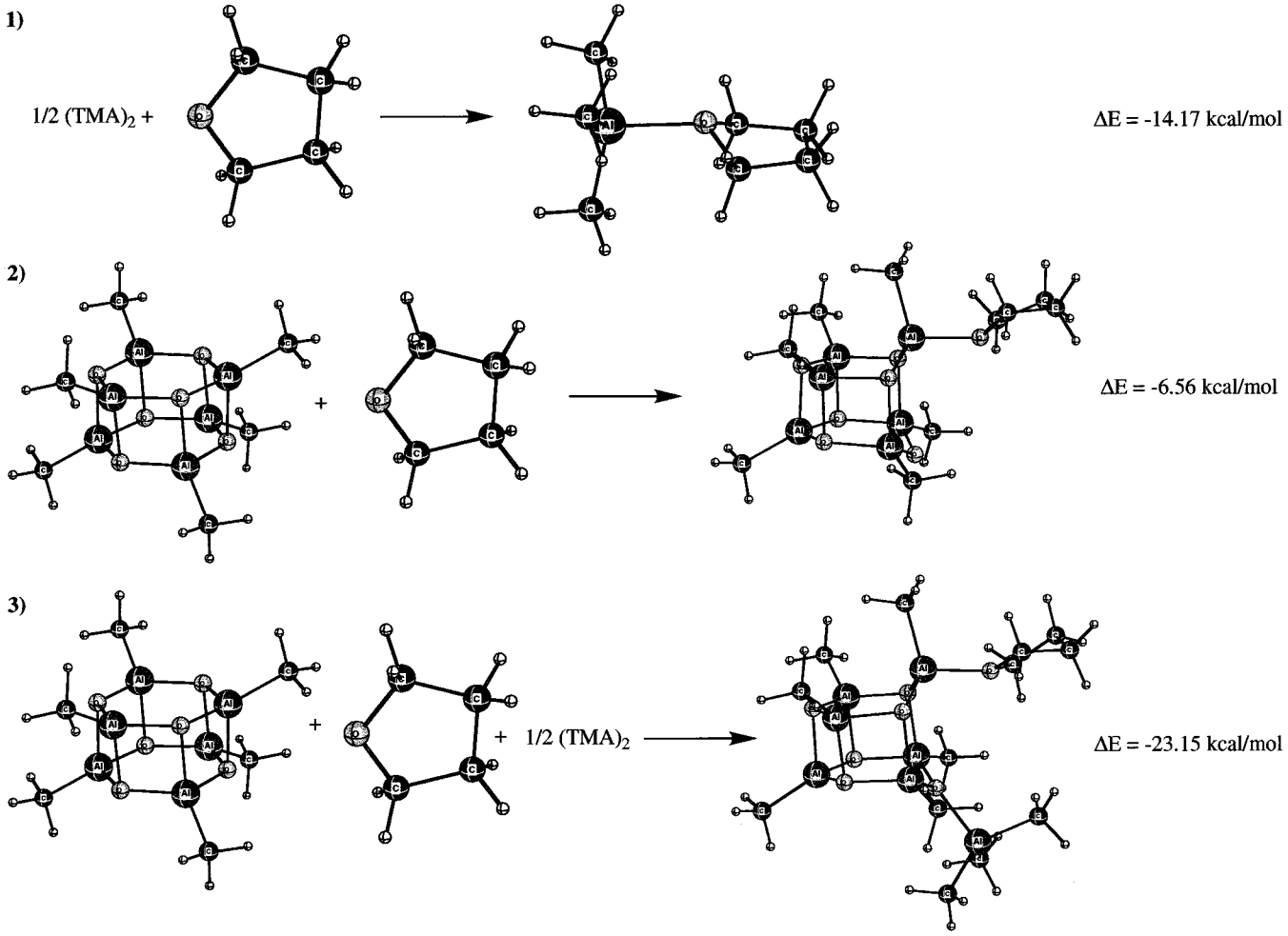

Figure 9. Reactions occurring in a $(AlOMe)_6$, TMA, and THF Mixture.

13 have been determined. With one exception, the most acidic sites consist of a bond belonging to two square faces with the corresponding O and Al atoms in a (2S + H) environment.

According to our calculations, it has been found that very little TMA is actually bound to MAO within the temperature range of 198.15−598.15 K. The addition of more than two TMA groups to a single MAO cage is energetically unfavorable due to increased steric hindrance of the ring-opened compound. Moreover, for $(AlOMe)_n$ structures where $n = 12$ or $n \geq 14$, the addition of even one single TMA group to the parent cage is energetically unfavorable. When finite temperature enthalpy corrections and entropies are taken into consideration, it is apparent that MAO cages are predominantly TMA free. The Me/Al ratio has been calculated as being 1.00, 1.01, 1.02, and 1.03 at 198, 298, 398, and 598 K. The percent of Al present as bound TMA of total TMA content has been calculated as being 0.21, 0.62, 1.05, and 1.76% for the aforementioned temperatures, with average unit formulas of $(AlOMe)_{18.08}\cdot(TMA)_{0.04}$, $(AlOMe)_{17.04}\cdot(TMA)_{0.11}$, $(AlOMe)_{15.72}\cdot(TMA)_{0.17}$, and $(AlOMe)_{14.62}\cdot(TMA)_{0.26}$. Somewhat more TMA is bound to the MAO cages at higher temperatures due to the fact that smaller structures are entropically more stable. Hence, parent cages with more Lewis acidic sites are in a greater abundance. Thus, even though the Gibbs free energy for the reaction **1** is not negative, the greater abundance of the parent cage increases the abundance of the TMA containing cage.

Our results do not agree with the experiment which finds a Me/Al ratio of approximately 1.5. However, we have shown that the errors present within our calculations should raise the Me/Al ratio to a maximum of 1.06 at 298 K. The errors which would have to be present in order to reach the "desired" ratio would have to be immense. We investigated the inclusion of solvation, finding that it did not change our values. We have also considered the presence of other bonding modes and concluded that they are not likely to occur. Finally, we have considered the experimental data showing that at least in one case, the assumptions present within the experiment were faulty and that it is likely that the method inflated the calculated Me/Al ratio. This result has also shown that the presence of basic impurities within the mixture ("dirty MAO") may have the effect of binding TMA to the MAO cages and furthermore lowering the average *n* value.

Acknowledgment. This study was supported by the Natural Science and Engineering Research Council of Canada (NSERC) and by Novacor Research and Technology (NRTC) of Calgary, Alberta, Canada. We would like to thank Dr. Clark Landis of the University of Wisconsin for supplying us with UFF2.

Supporting Information Available: Equations used to calculate thermodynamic properties; original and optimized UFF2 parameters; Cartesian coordinates of structures shown in Figures 3 and 4; Cartesian coordinates, energies, finite temperature enthalpy corrections, entropies, Gibbs Free Energies, and percent abundance at 198.15 K, 298.15 K, 398.15 K, and 598.15 K of 32 different $(AlOMe)_n\cdot(TMA)_m$ structures where *n* ranges between 6 and 13 ($n \neq 12$) and *m* between 1 and 4. This material is available free of charge via the Internet at http://pubs.acs.org.

IC001444Z